Neuron, Vol. 40, 733–748, November 13, 2003, Copyright ©2003 by Cell Press

Synaptojanin Is Recruited by Endophilin to Promote Synaptic Vesicle Uncoating

Patrik Verstreken,[1,2,6] Tong-Wey Koh,[2,6] Karen L. Schulze,[3] R. Grace Zhai,[3] P. Robin Hiesinger,[3] Yi Zhou,[1] Sunil Q. Mehta,[2] Yu Cao,[1] Jack Roos,[5,7] and Hugo J. Bellen[1,2,3,4,*]

[1]Department of Molecular and Human Genetics
[2]Program in Developmental Biology
[3]Howard Hughes Medical Institute
[4]Division of Neuroscience
Baylor College of Medicine
One Baylor Plaza
Houston, Texas 77030
[5]Department of Biochemistry and Biophysics
University of California, San Francisco
San Francisco, California 94143

Summary

We describe the isolation and characterization of *Drosophila synaptojanin (synj)* mutants. *synj* encodes a phosphatidylinositol phosphatase involved in clathrin-mediated endocytosis. We show that Synj is specifically localized to presynaptic terminals and is associated with synaptic vesicles. The electrophysiological and ultrastructural defects observed in *synj* mutants are strikingly similar to those found in *endophilin* mutants, and Synj and Endo colocalize and interact biochemically. Moreover, *synj; endo* double mutant synaptic terminals exhibit properties that are very similar to terminals of each single mutant, and overexpression of Endophilin can partially rescue the functional defects in partial loss-of-function *synj* mutants. Interestingly, Synj is mislocalized and destabilized at synapses devoid of Endophilin, suggesting that Endophilin recruits and stabilizes Synj on newly formed vesicles to promote vesicle uncoating. Our data also provide further evidence that kiss-and-run is able to maintain neurotransmitter release when synapses are not extensively challenged.

Introduction

Retrieval of the vesicular membrane and its associated proteins is an important step in maintaining a functional synaptic vesicle (SV) pool (Slepnev and De Camilli, 2000). Vesicles are retrieved by at least two mechanisms. One is clathrin-mediated endocytosis, which occurs at specialized zones following the full collapse of exocytotic vesicles, while another mode of vesicle retrieval is commonly termed "kiss-and-run" (Aravanis et al., 2003; Kjaerulff et al., 2002; Klyachko and Jackson, 2002; Sun et al., 2002). In kiss-and-run, SVs release their contents at the active zone (AZ) by forming a fusion pore that closes within fractions of seconds. Although stimulation frequency appears to modulate the release mode, the regulatory mechanisms are poorly understood (Sun et al., 2002; Verstreken et al., 2002).

Clathrin-mediated endocytosis is thought to be regulated by phosphoinositides in the presynaptic and vesicular membranes (Osborne et al., 2001). Phosphatidylinositol-4,5-bisphosphate (PI(4,5)P) may facilitate endocytosis by acting with endocytotic proteins, such as synaptotagmin I, to recruit AP2, AP180, and clathrin, leading to the formation of a clathrin-coated pit (Takei and Haucke, 2001). In addition, PI(4,5)P has been proposed to facilitate vesicle formation by recruiting epsin, a protein implicated in early steps of endocytosis and by stimulating the GTPase activity of dynamin, a protein required for vesicle scission (Hurley and Wendland, 2002). Finally, PI(4,5)P may affect vesicle transport by recruiting the actin polymerization machinery (Qualmann and Kessels, 2002; Sakisaka et al., 1997). Actin polymerization may provide a propulsive force to transport endocytosed SVs back to the AZ (Osborne et al., 2001), although this idea remains controversial (Sankaranarayanan et al., 2003). Thus, the phosphorylation status of the phosphosinositides likely plays an important role in regulating clathrin-mediated endocytosis.

Synaptojanin (Synj) is a polyphosphoinositide phosphatase (McPherson et al., 1996) that can bind proteins implicated in endocytosis, such as endophilin and Dap160/Intersectin (Ringstad et al., 1997; Roos and Kelly, 1998). Genetic disruption of the *Caenorhabditis elegans* homolog *unc-26* and mouse synaptojanin 1 leads to the accumulation of arrays of densely coated vesicles, suggesting that Synj functions in clathrin uncoating (Cremona et al., 1999; Harris et al., 2000). In the cortical neurons of *synaptojanin 1* knockout mice, vesicle recycling occurs at a slower rate but is not completely abolished (Kim et al., 2002). It remains unclear whether remaining endocytosis in the mouse *synaptojanin 1* mutant is the result of functional redundancy between the Synj homologs or compensation from different modes of vesicle retrieval.

We and others have previously characterized the function of Endophilin (Endo), a binding partner of Synaptojanin (Fabian-Fine et al., 2003; Gad, et al., 2000; Guichet et al., 2002; Rikhy et al., 2002; Ringstad et al., 1997; Verstreken et al., 2002). At the *Drosophila* neuromuscular junction (NMJ), *endo* null mutations lead to a general depletion of SVs, leaving small clusters of SVs at the AZs and a few densely coated vesicles in proximity of the presynaptic membrane (Verstreken et al., 2002). Dye-uptake assays with the fluorescent dye FM 1-43 indicate that the kiss-and-run mode of vesicle retrieval is retained in *endo* null mutants and that clathrin-mediated endocytosis is blocked. Furthermore, in photoreceptors (PR), loss of Endo leads to an accumulation of arrays of electron-dense vesicles that cannot enter the SV cycle. These data indicate an essential role for Endo late in endocytosis during SV uncoating (Fabian-Fine et al., 2003).

Here, we describe the isolation of *synaptojanin* mutants and present evidence that Synj acts during SV

*Correspondence: hbellen@bcm.tmc.edu
[6]These authors contributed equally to this work.
[7]Present address: Neurogenetics Inc., 11085 North Torrey Pines Road, Suite 300, La Jolla, California 92037.

uncoating. Interestingly, both *endo* and *synj* mutants as well as double mutants exhibit similar electrophysiological properties, ultrastructural anomalies, and behavioral phenotypes, suggesting that the two proteins are intimately linked during the uncoating process. This hypothesis is further supported by the colocalization of both proteins at synapses, by their biochemical interaction, and by the observation that overexpression of Endo partly rescues *synj* loss of function. Furthermore, our data suggest that a key function of Endo is to recruit and stabilize Synj on endocytosed vesicles.

Results

Isolation of Mutations that Affect Synaptic Transmission

We have performed a forward genetic screen to isolate mutations in genes involved in the SV cycle. Since mutations impairing synaptic function are likely to cause lethality, we used the *eyFLP* system to generate heterozygous mutant flies with homozygous mutant eyes (Newsome et al., 2000; Stowers and Schwarz, 1999). To enrich for flies with defects in synaptic transmission, we performed phototaxis assays (Benzer, 1967), allowing us to isolate flies with impaired sight.

To determine if synaptic transmission is affected in our mutants, we recorded electroretinograms (ERGs) (Heisenberg, 1971). ERGs distinguish between mutants that fail to perceive light (no depolarization in response to a light flash) and those that fail to elicit a postsynaptic response (reduced or absent on/off response). We therefore conducted ERGs on several flies in each stock and retained mutations that cause a defect in on and/or off transients.

The vast majority of the isolated mutations on chromosome arm 2R are homozygous lethal. To establish whether the mutations are allelic, we performed complementation tests based on lethality, assuming that lethality and the ERG defect are the result of the same mutation. This assumption proved to be correct in most cases. Our screen on 2R permitted isolation of 14 complementation groups with two or more alleles.

To assess ultrastructural defects in the mutants of each complementation group, we performed transmission electron microscopy (TEM) on PR terminals. *Drosophila* R1–R6 PRs project their axons into the first optic neuropil, the lamina, where they form synapses with monopolar cells, forming stereotypical cartridges (Meinertzhagen and Sorra, 2001). By combining the ERG and TEM data, we are able to pinpoint functional and structural defects in considerable detail.

Mutations in *2R11* Do Not Significantly Impair Phototaxis but Cause Lack of "On-Off" Transients

One of the complementation groups with two alleles ($2R11^1$ and $2R11^2$; later referred to as $synj^1$ and $synj^2$) displayed interesting phenotypes. ERG recordings on homozygous mutant *2R11* eyes, which appear morphologically wild-type, show a depolarization in response to light similar to controls (Figure 1A), suggesting that *2R11* does not impair the ability of the PRs to perceive light. However, these ERGs generally lack on/off transients (Figure 1A, gray arrowheads). Rarely, very small off transients can be observed (not shown). The abnormal on/off transients indicate that mutations in *2R11* impair the ability of PRs to signal to postsynaptic cells.

Since mutations that significantly affect synaptic transmission in PRs are expected to cause loss of phototaxis (Burg et al., 1993; Zinsmaier et al., 1994), we retested flies with homozygous mutant *2R11* eyes for phototaxis. Although *2R11* mutations were initially isolated in the screen because they displayed reduced positive phototaxis, when tested again, flies with homozygous mutant *2R11* eyes phototax as well as control flies in almost every trial (Figure 1B). Hence, *2R11* mutants are capable of detecting light and releasing sufficient neurotransmitter to display phototaxis.

Postsynaptic response defects measured by ERGs could arise from defects in neurotransmitter release but also from a failure of the mutant PRs to synapse with the correct postsynaptic cells. To determine the axonal morphology of the mutant PRs, we labeled PRs with a membrane-specific marker (mAb 24B10) and visualized their axon projection pattern by confocal microscopy. Detailed analysis of the projection patterns of mutant and control PRs did not reveal any obvious differences (data not shown). In addition, transmission electron microscopy (TEM) on the lamina of flies with *2R11* mutant PRs revealed that they sort in the usual stereotypical manner into lamina cartridges (Figures 1C–1E). Hence, mutations in *2R11* do not affect synaptic transmission by impairing PR axon pathfinding, target recognition, or sorting into lamina cartridges.

2R11 Mutant Photoreceptor Terminals Display Highly Clustered and Densely Coated Synaptic Vesicles

Although we did not observe gross morphological defects by TEM, there was an obvious difference between control and *2R11* mutant terminals. In both $2R11^1$ as well as in $2R11^2$ mutant PRs, SVs appear dense and cluster in highly organized rows (Figures 1G and 1H and insets), a phenotype we never observed in control terminals (Figure 1F). Other subcellular structures do not exhibit obvious defects when compared to control terminals. Hence, *2R11* mutants display highly organized densely coated vesicles in contrast to the less conspicuous and more dispersed SVs of controls, suggesting a defect in vesicle uncoating and cytoskeletal organization. Since the ERG, phototaxis, and ultrastructural phenotypes of *2R11* are very similar to those observed in *endo* mutant PRs (Fabian-Fine et al., 2003), we studied *2R11* in more detail.

2R11 Corresponds to *synaptojanin*

To map the *2R11* complementation group, we determined the recombination distance between the mutations and nine P element insertions spread over the 2R chromosome arm (Zhai et al., 2003). As shown in Figure 2A, both mutations map at cytological interval 58. Using four different P elements within this interval (Figure 2B) as well as deficiency complementation testing (Figure 2C), we refined the mapping position to a region of less than 20 ORFs (Figure 2D). The most obvious candidate gene in this region is *synaptojanin* (*synj*) (Lloyd et al., 2000), whose gene product has been implicated in SV

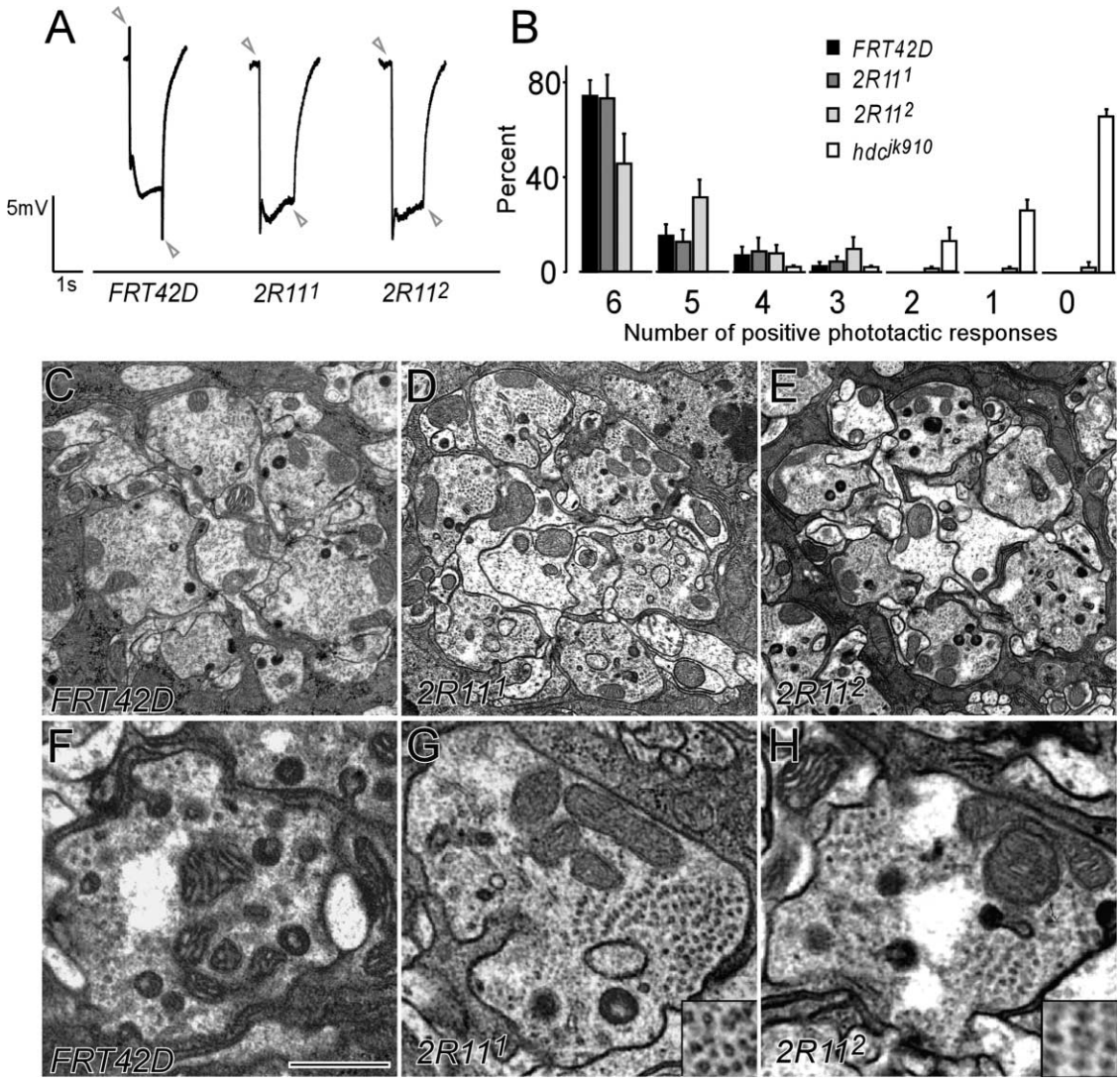

Figure 1. Synaptic Function in *2R11* Mutant Photoreceptors Is Impaired

(A) ERGs from control *y w eyFLP; FRT42D/FRT42D cl2R* w^+, $2R11^1$, and $2R11^2$ mutant eyes (genotype: *y w eyFLP; FRT42D* $2R11^{1\ or\ 2}$*/FRT42D cl2R* w^+). Positions of on and off transients are marked by arrowheads.

(B) Countercurrent phototaxis assay on control flies and flies with homozygous $2R11^1$ and $2R11^2$ eyes. hdc^{jk910} flies lack histamine in their PRs and serve as a negative control. Flies were allowed to phototax in seven trials, and the average percentage of flies that displayed positive phototaxis for the indicated number of times is plotted.

(C–E) TEM of lamina cartridges of control (C), $2R11^1$ (D), and $2R11^2$ (E) eyes. Sorting of PRs into cartridges is normal in the mutants.

(F–H) PR terminal profiles of control (F), $2R11^1$ (G), and $2R11^2$ (H) mutants. Organized darkly coated SV clusters can be observed in $2R11^1$ and $2R11^2$ mutant PR terminals. Scale bar equals 900 nm in (C)–(E) and 500 nm in (F)–(H).

endocytosis (Cremona et al., 1999; Harris et al., 2000; McPherson et al., 1996). *Drosophila* Synj contains an N-terminal Sac-1 inositol-phosphatase (InsP) domain, a central Ins-5-P domain, and a C-terminal proline-rich domain, which are 69%, 73%, and 28% similar to the rat Synaptojanin domains, respectively (Figure 2F). The fly genome encodes one protein harboring this domain structure. We sequenced *synj* in both mutants and found a CAG-to-TAG nonsense mutation at amino acid 460 in $2R11^1$ and a GGT-to-GAT missense mutation leading to a G-to-D substitution at amino acid 65 in $2R11^2$. From this point on, we refer to $2R11^1$ as $synj^1$ and to $2R11^2$ as $synj^2$ (Figures 2E and 2F). To determine if the lesions in $synj^1$ and $synj^2$ are responsible for the lethality and phenotypes associated with the mutants, we used two cosmids, each containing the entire $synj^+$ gene (Kerrebrock et al., 1995; see Experimental Procedures). Cosmid$^{1-12}$ and cosmid$^{1-5}$ (Figure 2D) were able to rescue the lethality and restore the on and off transients of ERG recordings of $synj^1/synj^2$, $synj^1/synj^1$, and $synj^2/synj^2$ animals (not shown). Hence, *2R11* corresponds to *synj*.

$synj^1$ and $synj^2$ homozygous animals as well as $synj^1$/*Df(2R)R1-8*, $synj^2$/*Df(2R)R1-8*, and $synj^1/synj^2$ larvae move slowly, become paralyzed, and die as third instar larvae or early pupae. However, compared to $synj^2$/*Df(2R)R1-8*, somewhat fewer $synj^1$/*Df(2R)R1-8* larvae survive until the early pupal stage. Hence, based on their lethal phase, both $synj^1$ and $synj^2$ are likely strong loss-

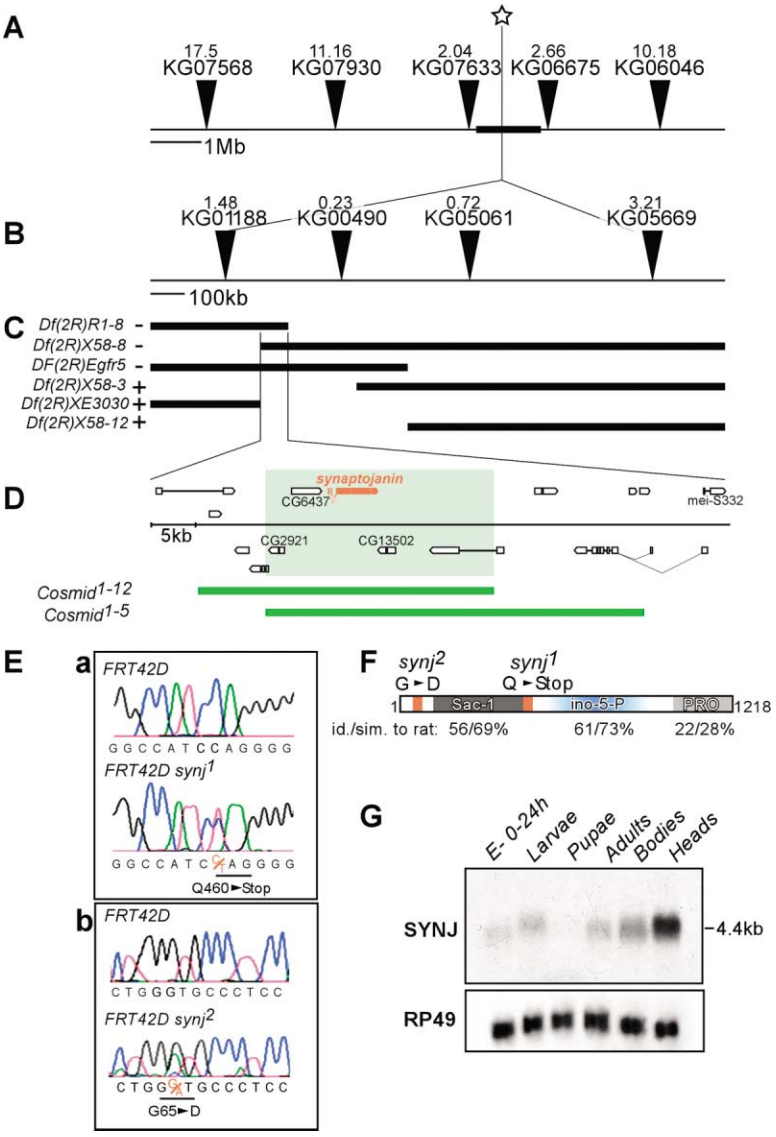

Figure 2. Identification of Mutations in *synaptojanin*

(A) Recombination mapping using P element insertions localizes *2R11* between KG07633 and KG06675 insertions. The recombination distances between the insertion and the mutation were calculated from counting at least 7000 flies and are indicated above the name of the insertion.

(B and C) Recombination mapping in the region indicated by a bold bar in (A) using four new P element insertions. Deficiency complementation mapping localized the mutations to a small interval (C).

(D) Mapping interval with ORFs; the most obvious candidate is *synaptojanin*, indicated in red. Overlapping genomic fragments in cosmid$^{1-12}$ and cosmid$^{1-5}$ rescue the *synj* phenotypes. Cosmid breakpoints were mapped by Southern and sequencing. The overlap between both cosmids in the light green box contains only four genes.

(E) Sequencing of heterozygous (*FRT42D synj/FRT42D^{iso}*) *synj* alleles reveals a stop codon at amino acid position 460 in *synj^1* (a) and a G65D substitution in *synj^2* (b).

(F) Synj protein structure. Synj contains a Sac-1 InsP domain that is predicted to hydrolyze PI(3)P (phosphatidyl inositol-3-phosphate), PI(4)P, and PI(3,5)P to PI in vitro; a central Ins-5-P domain that is predicted to act on PI(4,5)P and on PI(3,4,5)P; and a C-terminal proline-rich domain. Lesions in *synj^1* and *synj^2* are indicated in red.

(G) Developmental Northern blot of *SYNJ* and control (ribosomal protein RP49).

of-function alleles, *synj^1* being somewhat more severe than *synj^2*.

Synaptojanin Is a Presynaptic Protein Associated with Vesicles

To determine the developmental expression profile of *synj*, we performed a developmental Northern blot (Figure 2G). One broad band is detected at 4.4 kb, corresponding to the predicted size of the *synj* transcript. *SYNJ* message is low during embryonic stages and absent during pupal stages. RNA expression is observed in larvae and adults, especially in adult heads (Figure 2G).

To determine the localization of Synj, we produced a rabbit antiserum against the proline-rich domain. Immunohistochemical staining shows strong labeling of all types of boutons of the third instar larval neuromuscular junction (NMJ) in controls (Figure 3A) but not at *synj^1/Df(2R)R1-8* NMJs (Figure 3C), demonstrating that the antiserum is specific. *synj^1/synj^2* (Figure 3B) and *synj^2/synj^2* (not shown) NMJs show severely reduced labeling, indicating that Synj protein expression is reduced or that the protein is unstable in *synj^2* mutants.

We also labeled staged embryos and larvae with the Synj antiserum and detected very faint or no labeling in stage 15 embryos. Neuropil-specific labeling is first detected in stage 16–17 embryos and is more apparent in the neuropils of first instar larvae, third instar larvae, and adult brains (not shown, Figures 3D and 3E). To determine if Synj is present in synaptic terminals of PRs, we stained them with anti-Synj and the PR cell membrane marker anti-chaoptin (mAb 24B10, Figure 3F; Van Vactor et al., 1988). The Synj antiserum stains cartridges in the lamina and extensively labels the R1-R6 PR terminals (Figures 3F and 3G), indicating that Synj is enriched in synaptic contact sites.

To establish the distribution of Synj at the synapse, we labeled larval NMJs using anti-Synj and various synaptic markers. Synj is contained within the domain labeled by anti-DVAP-33, a pre- and postsynaptic marker (Figure

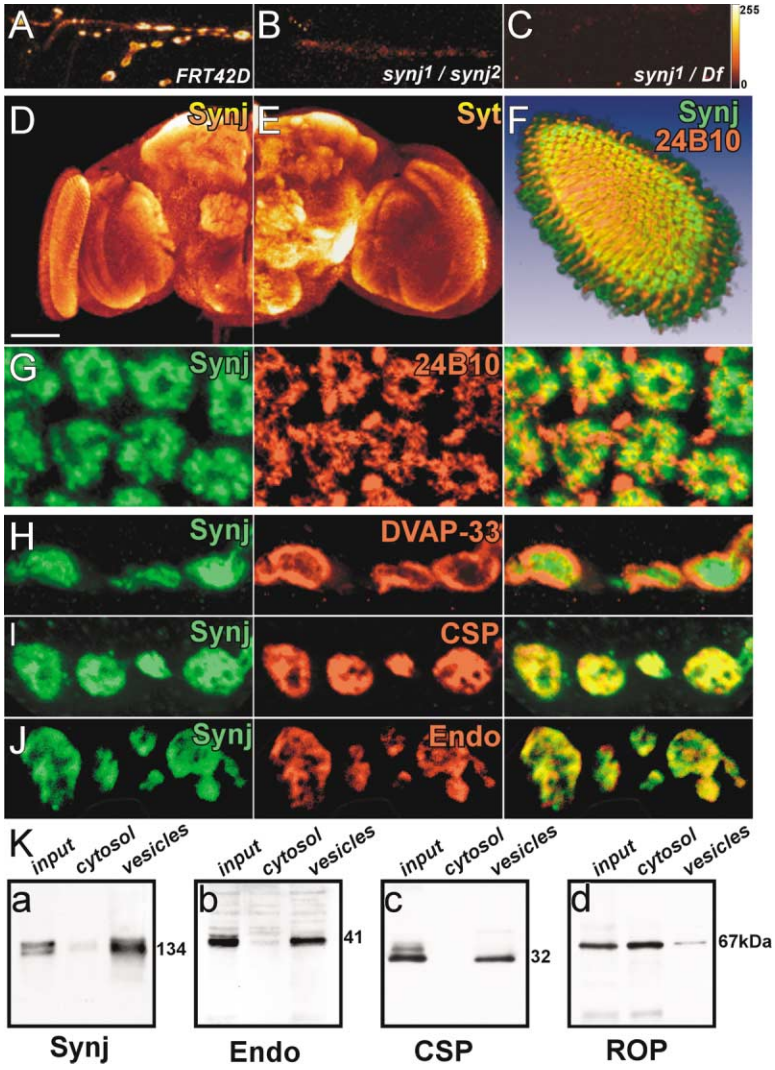

Figure 3. Synaptojanin Is Present in Boutons of the NMJ and in Photoreceptor Terminals

(A–C) Labeling of control *y w; FRT42D* (A), *y w eyFLP; FRT42D synj*^{2}*/FRT42D synj*^{1} (B), and *y w eyFLP; FRT42D synj*^{1}*/Df(2R)R1-8* (C) NMJs with Synj antiserum. Labeling is detected at all types of boutons (A) but is reduced in *FRT42D synj*^{1}*/FRT42D synj*^{2} and is not detected at *FRT42D synj*^{1}*/Df(2R)R1-8* NMJs.

(D and E) Adult brain labeling (*y w; FRT42D*) with Synj antibodies (D) and SytI antibodies (E) shows, similar to Syt, enrichment of Synj in the neuropil.

(F) Three-dimensional representation of a lamina double-labeled with Synj and 24B10. Synj is present in the neuropil-rich area and extensively colocalizes with the PR marker 24B10.

(G–J) Single confocal sections of double-labeled boutons/synapses with Synj and 24B10 (G), DVAP-33A (H), CSP (I), or Endo (J). 24B10 and Synj colocalize extensively (G). The bright red labeling next to each cartridge corresponds to the axons of R7 and R8 PRs. Synj is a presynaptic marker (H and I) and extensively colocalizes with Endo (J); however, Endo localization appears somewhat more restricted than that of Synj.

(K) Subcellular distribution of Synj and Endo. Synj (a) is mostly associated with vesicle membranes; Endo and the vesicular marker CSP are also mostly associated with vesicles (b and c), whereas ROP, a vesicle cycle regulatory protein, is mostly present in the cytoplasm (d).

3H; Pennetta et al., 2002), and largely overlaps with the presynaptic vesicle-associated protein CSP (Figure 3I; Zinsmaier et al., 1994). Finally, Synj colocalizes extensively with Endo (Figure 3J). Hence, Synj is localized presynaptically at the motor neuron synapse.

To assess the subcellular distribution of Synj, we fractionated fly head extract using sucrose density step centrifugation and probed for the presence of Synj and various markers (Figure 3K; Schulze et al., 1995). Vesicle markers CSP and Synaptobrevin are detected specifically in the vesicle fraction, while the cytoplasmic proteins ROP and Drab3A are found in both the cytosolic and vesicular fractions (Figure 3K, c and d, and data not shown). Synj is present at low levels in the cytosol but is significantly enriched in the SV fraction, similar to the subcellular distribution of Endo (Figure 3K, a and b; Fabian-Fine et al., 2003). However, as the vesicle fraction may contain plasma membrane contaminants, we do not rule out the possibility that some Synj or Endo is plasma membrane associated. Nonetheless, these findings strongly suggest that Synj and Endo are mostly vesicle associated, in agreement with the immunohistochemical data.

Endocytosis Is Impaired in *synj* Mutants

To determine if Synj is involved in exocytosis, we stimulated the motor neurons and recorded the excitatory junctional potential (EJPs) of abdominal muscles. The EJPs in *synj*^{1}*/synj*^{2}, *synj*^{1}*/Df(2R)R1-8*, and *synj*^{2}*/Df(2R)R1-8* animals are not significantly different from controls (Figures 4A and 4B). Hence, Synj does not affect exocytosis of neurotransmitters in this paradigm.

To reveal defects in vesicle cycling, we repetitively stimulated motor neurons and monitored the amplitude of the EJP over time. At low-frequency stimulation (1 Hz), the EJP amplitude of controls and *synj* mutants declined marginally, and they were similar after 10 min of stimulation (Figure 4C). Strikingly, at higher-stimulation frequency (10 Hz), the amplitude of the EJP measured from *synj* mutants rapidly declines to about 25%–30% of the original response and is then maintained during the remainder of the paradigm (Figures 4D and 4E). Hence, at low-frequency stimulation, *synj* mutants maintain neurotransmitter release similar to controls, whereas in a high-frequency paradigm, *synj* mutants show a severe impairment in vesicle release. These data suggest that vesicle recycling is disrupted in *synj* mutants.

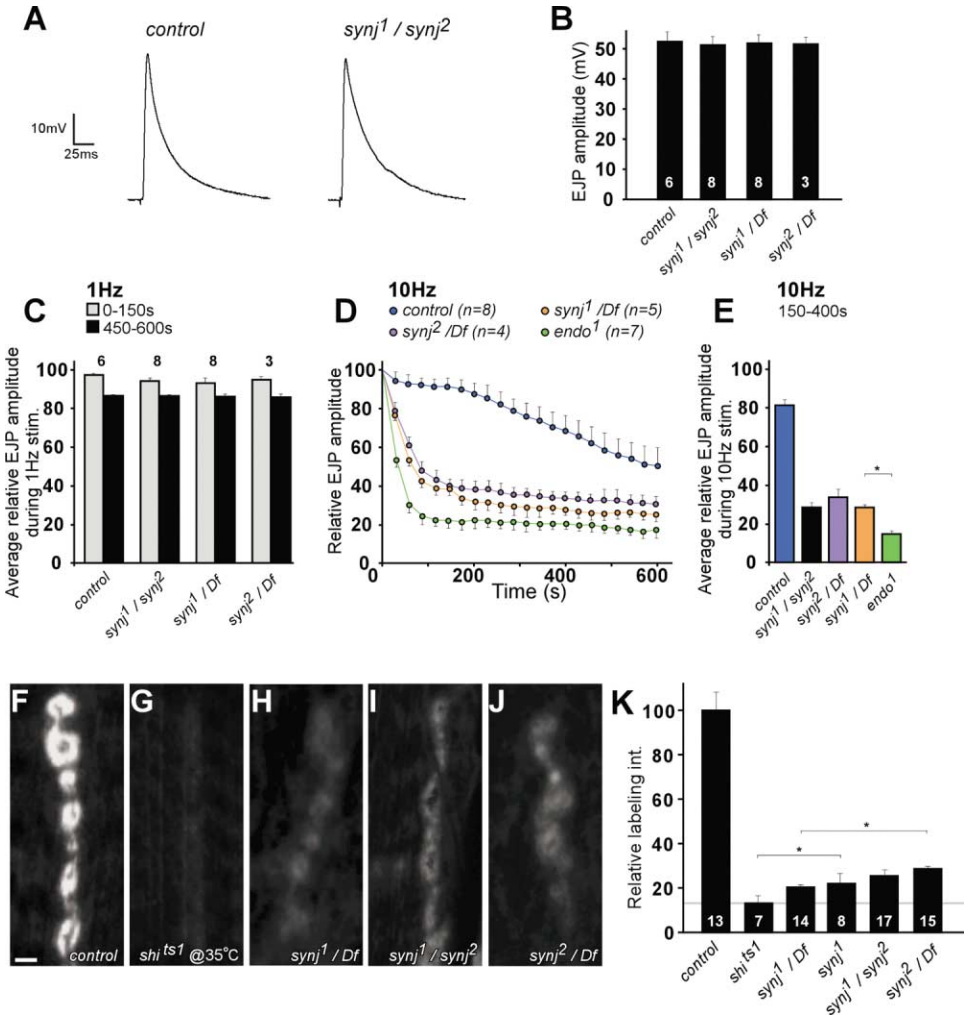

Figure 4. *synanptojanin* Mutants Maintain Neurotransmitter Release at Low- but Not at High-Frequency Stimulation

(A–C) Neurotransmitter release is not affected at low-frequency stimulation in *synj* mutants.

(A) Example of traces recorded from muscle 6 in abdominal segment 2 of control (*y w; FRT42D*) and $synj^1/synj^2$ mutants (*y w eyFLP; FRT42D* $synj^1$/*FRT42D* $synj^2$).

(B) Quantification of EJP amplitude in controls and different *synj* mutants.

(C) Stimulation at 1 Hz for 10 min. EJP amplitude during the first 150 s was averaged and is reported as a fraction of control (gray bars). The average relative EJP amplitude during the last 150 s of the stimulation paradigm (450–600 s) is shown in black bars. The modest decline in EJP amplitude in mutants is not significantly different from controls.

(D and E) The EJP amplitude in *synj* mutants during high-frequency stimulation (10 Hz for 10 min) rapidly declines but stabilizes at a low level.

(D) Average relative EJP time course during 10 Hz stimulation for control (blue), $synj^2$ (purple), $synj^1$ (orange), and $endo^1$ (green; *w;* $endo^1$). The EJP rapidly declines in *synj* and in $endo^1$ mutants but is then maintained at a steady level.

(E) The level at which neurotransmitter release is maintained at 10 Hz in different *synj* mutants and in $endo^1$ was quantified by determining the average relative EJP amplitude between 150 and 450 s of stimulation. The EJP is maintained at 36.7% of the original level in $synj^2$/*Df(2R)R1-8*, at 28.9% in $synj^1/synj^2$, at 29.0% in $synj^1$/*Df(2R)R1-8*, and at 20.0% in $endo^1$ (*$p < 0.01$).

(F–K) FM1-43 dye uptake is severely reduced in *synj* mutants.

(F–J) Filleted larvae were incubated for 10 min in HL3 with 60 mM potassium and FM1-43. Robust labeling is observed in controls (*y w; FRT42D* at room temperature or at 35°C) (F) and is virtually absent in shi^{ts1} animals at the restrictive temperature (35°C) (G). Uptake of dye in *synj* mutants (genotypes, see A) is severely reduced (H and I). Dye uptake is plotted as a percentage of labeling in controls (K). Labeling is significantly different in shi^{ts1} versus *synj* mutants, and labeling in $synj^1$/*Df(2R)R1-8* is significantly different from labeling in $synj^2$/*Df(2R)R1-8* (*$p < 0.01$),

(B, C, and K) Number of animals tested is indicated in the bars.

Error bars indicate SEM.

Interestingly, $endo^1$ mutants exhibit a very similar phenotype during 10 Hz stimulation (Verstreken et al., 2002). While $synj^1$ mutants maintain release at 25%–30% during 10 Hz stimulation, $endo^1$ mutants maintain release at 20% (Figures 4D and 4E). These data suggest that SV recycling at the NMJ is disrupted somewhat more severely in $endo^1$ mutants than in $synj^1$ mutants.

To test for defects in SV retrieval more directly, we analyzed uptake of FM1-43, a fluorescent lipophilic dye that is internalized by endocytosis (Betz and Bewick,

1992). Filleted larvae were incubated for 10 min in FM1-43 and stimulated with 60 mM potassium. In control animals, dye is readily internalized into vesicles at synaptic boutons (Figures 4F and 4K; 100 ± 7.4 arbitrary units [a.u.]), whereas in *shibire^{ts1}* mutants (*shi^{ts1}*) where Dynamin function is blocked at high temperature, FM1-43 uptake is essentially abolished (Figures 4G and 4K; 12.9 ± 4.0 a.u.). Labeling in *synj^{1}*/*synj^{1}* and in *synj^{1}*/*Df(2R)R1-8* are both reduced by 80% compared to controls (20 ± 0.8 a.u. and 22 ± 3.9 a.u., respectively), consistent with *synj^{1}* being a severe loss-of-function mutation. Uptake in *synj^{2}*/*Df(2R)R1-8* is less severely reduced: 28.3 ± 1.3 a.u. ($p < 0.01$ compared to *synj^{1}*/*Df(2R)R1-8*) (Figures 4H–4K). In summary, the data indicate that mutations in *synj* dramatically impair endocytosis.

Synaptic Vesicles Are Largely Depleted from *synj* Mutant NMJ Boutons, but Darkly Coated Vesicles Remain

To correlate the physiological defects observed at NMJs with structural defects, we performed TEM on NMJ boutons (Figures 5A–5J). SVs are largely depleted from synaptic boutons of *synj^{1}* terminals (Figures 5B and 5K), whereas *synj^{2}* animals exhibit a less severe depletion (Figure 5K). In *synj^{1}* boutons, small numbers of SV remains in two locations: (1) the AZ and (2) in discrete areas outside the AZs (Figures 5B–5H). The non-AZ vesicles are close to the synaptic membrane and often appear densely coated, reminiscent of clathrin-coated vesicles. Other organelles, including cisternae, are not dramatically different between controls and *synj* mutants ($p > 0.01$; Figure 5L). These data further support a role for Synj in vesicle endocytosis.

Synaptojanin and Endophilin Interact In Vitro and In Vivo

Studies of rat Synj indicate proline-rich domain-mediated interactions with endocytotic proteins such as Endophilin and Dap160/intersectin (Ringstad et al., 1997; Roos and Kelly, 1998). The *Drosophila* Synj proline-rich domain (SynjPRD) shows only 22% sequence identity to that of rat Synj. We therefore determined whether the *Drosophila* SynjPRD interacts with Endo, Dap160, or Dynamin by performing a GST pull-down experiment. We found that GST-SynjPRD interacts with Endo and Dap160, but not with Dynamin or the vesicular marker n-Syb (Figure 6A). We confirmed the interaction of Endo and Synj by immunoprecipitation (IP) using anti-Endo antibodies on fly head extracts (data not shown).

To substantiate the interaction of Dap160 and Synj, we performed GST pull-down experiments on fly head extracts using the four SH3 domains (SH3-A-D) of *Drosophila* Dap160. Synj binds tightly to the Dap160C-D-SH3 domains and it binds with lower affinity to the SH3-C domain (Figure 6B). Notably, Synj does not bind to the other SH3 domains in isolation or to combinations of SH3 domains. Dynamin also binds to Dap160 SH3 domains, including the SH3-C-D domain, but Dynamin does not bind to Dap160 SH3-C, which interacts with Synj (Figure 6B; Roos and Kelly, 1998). Hence, the data suggest that the four SH3 domains of Dap160 play different roles. While Dap160 SH3-C binds Synj, the SH3 B domain appears inhibitory and SH3-D appears to promote Synj binding. In addition, Dap160 interacts with Dynamin and Synj at different sites, suggesting that Dap160 can bind Dynamin and Synj simultaneously.

Vesicle depletion experiments with *shi^{ts1}* show a relocalization of synaptic proteins to endocytotic zones at the plasma membrane (Koenig and Ikeda, 1989; van de Goor et al., 1995). To determine if Synj also relocalizes in vesicle-depleted terminals, we incubated *shi^{ts1}* larvae at the restrictive temperature (35°C, 20 min). This treatment is known to deplete the SV pool (van de Goor et al., 1995). *shi^{ts1}* animals were then fixed and labeled with Synj and Endo antisera. Similar to Endo and α-adaptin (Gonzalez-Gaitan and Jackle, 1997; Guichet et al., 2002), Synj also relocalizes somewhat to the synaptic membrane upon vesicle depletion (Figure 6C).

To test if the interaction of Endo with Synj depends on the presence of SVs, we performed IP experiments with anti-Endo antibodies on head extract of *shi^{ts1}* animals held at 35°C for 20 min. Interestingly, we found slightly more Synj interacting with Endo after vesicle depletion as compared to prior to depletion (Figure 6D), suggesting that Endo and Synj are able to associate with each other in the absence of SVs. In summary, the data presented here show that Synj interacts with Endo and Dap160, but likely not with Dynamin.

synj; endo Double Mutants Exhibit Phenotypes Similar to Each Single Mutant

To further test if Endo and Synj function in the same process, we created heterozygous flies with double mutant *synj* and *endo* eyes. *synj^{1}*; *endo^{1}* eyes develop normally; however, the on/off transients in ERG recordings are absent in double mutant eyes (Figure 7A), similar to our findings with *synj^{1}* and *endo^{1}* single mutant eyes (Figure 1A; Fabian-Fine et al., 2003). In addition, similar to the single mutants, flies with double mutant eyes phototax properly (Figure 7B), indicating that some neurotransmitter release persists even in the absence of both normal Endo and Synj function.

To determine the vesicle morphology of *synj^{1}*; *endo^{1}* mutant PR terminals, we performed TEM on lamina cross-sections (Figures 7C–7F). PRs double mutant for *synj^{1}* and *endo^{1}* form normal cartridges in the lamina (not shown); however, similar to the vesicle clusters found in *synj^{1}* and *endo^{1}* mutant PR terminals, rows of densely coated vesicles accumulate in double mutant PR terminals (Figures 7D–7F; Fabian-Fine et al., 2003). Comparison of vesicle cluster size in single and double mutants did not reveal a significant difference ($p > 0.01$), suggesting that the effects of *endo* and *synj* mutations are not additive in PRs.

To test if *synj^{1}*; *endo^{1}* double mutants also behave similarly to each single mutant at the NMJ, we monitored the persistence of neurotransmitter release during intense stimulation. Interestingly, EJPs in double mutants stimulated at 10 Hz rapidly decline and maintain a low level of release for at least 10 min, very similar to *endo^{1}* mutants (Figure 7G). Averaging relative EJP amplitudes recorded between 150 s and 400 s of 10 Hz stimulation reveals no difference between *endo^{1}* single (20%) and *synj^{1}*; *endo^{1}* double mutants (19%; Figure 7H; $p > 0.01$). Hence, the similar phenotypes of *synj^{1}* and *endo^{1}* single

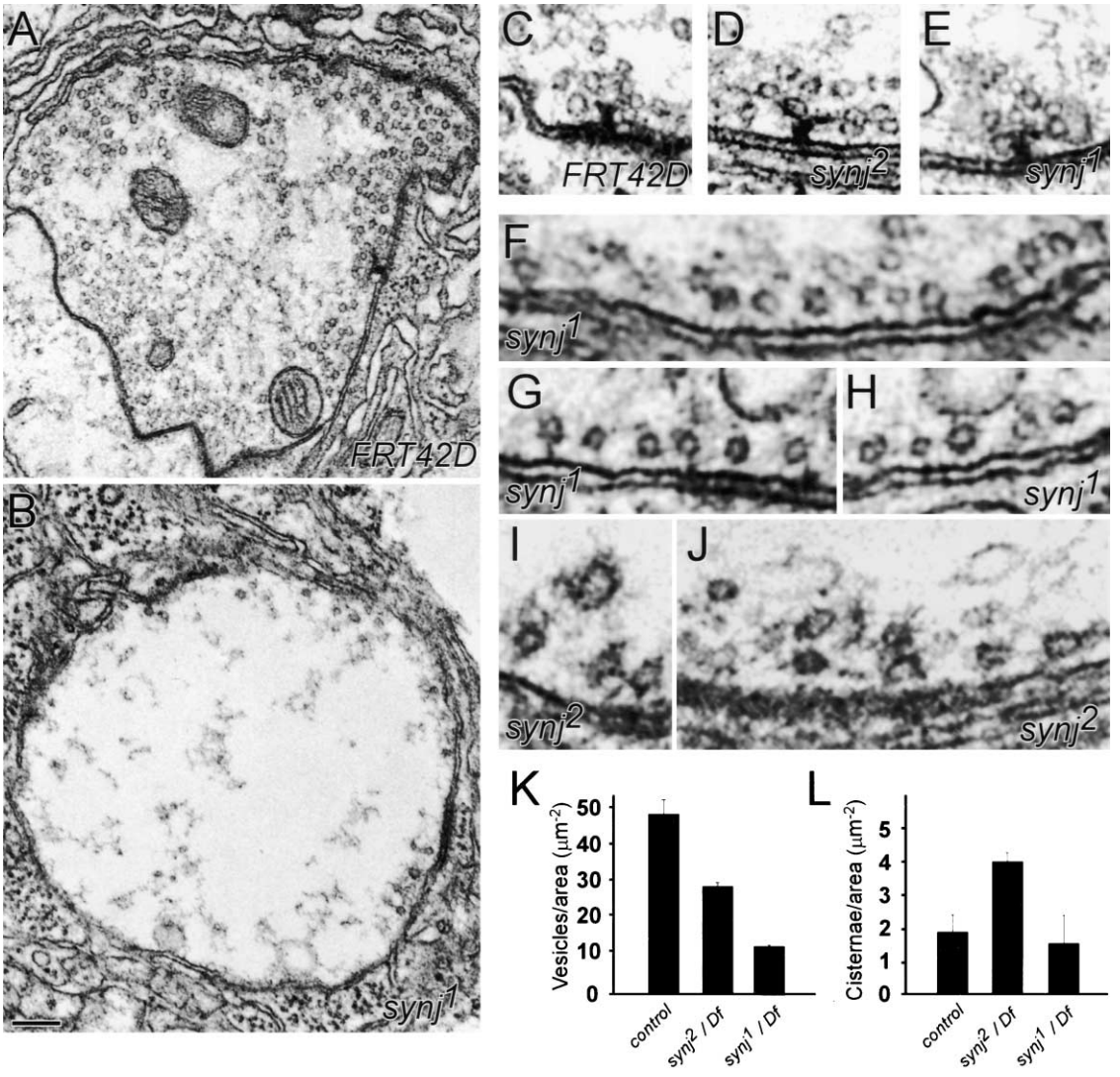

Figure 5. Boutons of *synj* NMJs Are Severely Depleted of Synaptic Vesicles

(A and B) Electron micrographs of type I boutons of control (A) (*y w; FRT42D*) and *synj*^{1} (B) (*y w eyFLP; FRT42D synj*^{1}).

(C–E) High magnification of AZs in control (C), *synj*^{2} (D) (*y w eyFLP; FRT42D synj*^{2}), and *synj*^{1} (E) synapses. Note the clear SVs associated with the AZ in control and mutant NMJ boutons.

(F–J) High magnification of darkly coated vesicles in proximity of the plasma membrane in *synj*^{1} (F–H) and *synj*^{2} (I and J). Scale bar equals 0.2 μm for (A) and (B), 95 nm for (C)–(E), and 90 nm for (F)–(J).

(K and L) Quantification of vesicle density (K) and cisternae density (L) in control and mutant type I boutons. Vesicles were counted from at least 10 bouton sections from 3 different animals per genotype ($p < 0.01$ for all genotypes). Cisternae densities in the different genotypes are not significantly different ($p > 0.01$ for all genotypes). Error bars indicate SEM.

mutants and the double mutants at PR terminals and at NMJs provide further evidence that Synj and Endo function in the same process.

Overexpression of Endo Partially Rescues Loss of Synj Function

To determine if additional Endo can alleviate the functional defects associated with partial loss of *synj* function, we overexpressed Endo in *synj* mutant PRs. ERG recordings starting with "lights on," performed on eyes that overexpress Endo, are normal in response to repetitive light flashes (500 ms) (Figures 8A, arrowheads, and 8F). In contrast, on/off transients are largely absent from ERG recordings made from *synj*^{2} or *synj*^{1} eyes (Figures 8B, 8D, and 8F). However, occasionally a small and delayed off transient is observed in *synj*^{2} and to a lesser extent in *synj*^{1} (Figures 8B, 8D, and 8F, inset). Interestingly, when Endo is overexpressed in hypomorphic *synj*^{2} mutant PRs, where low levels of Synj protein are still detected at the synapse (Figure 3B), the timing and the amplitude of the off transient are partially rescued (Figures 8C and 8F). Overexpression of Endo in the stronger *synj*^{1} mutant PRs only weakly rescues the off transient (Figures 8E and 8F). Hence, Endo overexpression is capable of partially compensating the functional defects associated with reduced *synj* function.

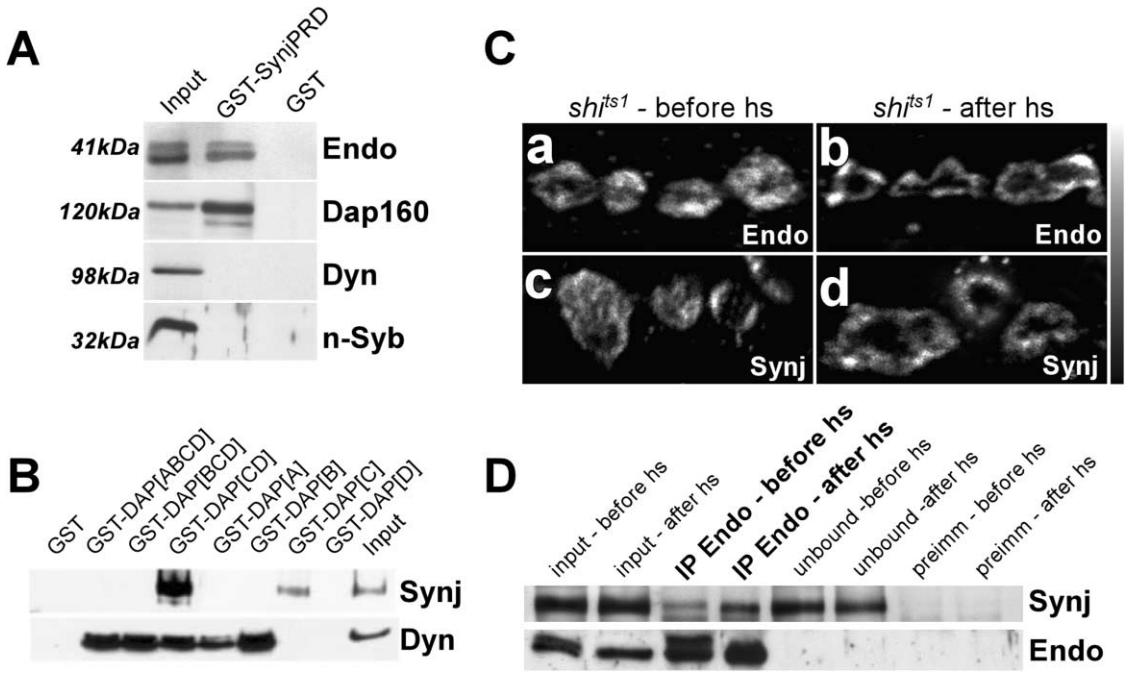

Figure 6. Synj Interacts with Endo and Dap160

(A) GST pull-down with the proline-rich domain of *Drosophila* Synj (GST-SynjPRD) from *Drosophila* head extract. GST-SynjPRD binds to Endo and Dap160, but not to Dynamin (Dyn) or neuronal Synaptobrevin (n-syb).

(B) GST pull-down experiment with the SH3 domains of *Drosophila* Dap160. Dap160 has four SH3 domains "A"–"D," and the SH3 domains that were included are indicated. Synj interacts with the SH3 C and D domains and with the SH3 C domain of Dap160 in isolation. Dynamin interacts with the SH3 ABCD, BCD, and CD domains and with the SH3 A and B domains, but not with the C domain in isolation.

(C) Synj and Endo relocalize to the membrane upon vesicle depletion. (a and c) Single confocal sections of NMJ boutons of *shibire^{ts1}* larvae at the permissive temperature, before heat shock, labeled with anti-Endo (a) or anti-Synj (c). (b and d) Single confocal sections of NMJ boutons of *shibire^{ts1}* larvae exposed to the restrictive temperature (35°C) (after heat shock), labeled with anti-Endo (b) or anti-Synj (d). Both markers partialy relocalize to the membrane after heat shock treatment.

(D) IP on head extract of *shi^{ts1}* animals before or after a 20 min heat shock at 35°C. Incubation and loading was normalized against the amount of Endo protein (bottom blot). We also verified that all the Endo was precipitated from the head extract under these conditions (bottom blot "unbound before hs and after hs"). This ensures that we are assessing the total amount of Endo-Synj complexes before and after vesicle depletion. More Synj is bound to Endo after heat shock (top blot, "IP endo before and after heat shock").

To correlate the partial rescue of ERG defects with ultrastructural defects, we performed TEM on *synj^2* PR terminals. The sorting of PRs into lamina cartridges is normal in PRs overexpressing Endo and *synj^2* mutant PRs that overexpress Endo (not shown), indicating that axon guidance and targeting into cartridges in these genotypes is not altered. Unlike vesicles at *synj^2* PR terminals (Figure 8H), vesicles at terminals that overexpress Endo are not densely coated and arranged in clusters (Figure 8G). Interestingly, in *synj^2* PR terminals that overexpress Endo, large clusters of densely coated vesicles are present and are more apparent than in *synj^2* mutants (Figure 8I, arrowheads). These vesicles may serve as substrates for the remaining Synj protein in *synj^2* mutants, allowing a small number of vesicles to proceed through the vesicle cycle, thereby leading to the partial rescue of the ERG response.

Synaptojanin Levels Are Reduced and the Remaining Synaptojanin Is Localized to Endocytotic Hotspots in *endo* Mutants

To investigate in vivo interaction between Endo and Synj, we labeled *synj^1* and *endo^1* mutant boutons with endocytotic markers. Dynamin and Dap160 are localized similarly in control and mutant boutons, indicating that their localization is not dependent on Synj or Endo (Figures 9A–9F). However, Synj is strikingly relocalized in *endo^1* mutants to the periphery of the boutons and appears in a punctate pattern (Figures 9G and 9H). In addition, Synj immunoreactivity is dramatically reduced in *endo^1* mutants (Figures 9H and 9I), indicating that Synj expression at the synapse depends on Endo. In contrast, Endo is only partially relocalized to the membrane in *synj^1* mutants, indicating that Endo localization is not critically dependent on Synj (Figures 9J and 9K).

To test if the reduced Synj protein in *endo^1* boutons is a result of decreased Synj expression, of decreased Synj transport to the NMJ, or of destabilization and degradation of the protein, we determined Synj protein and RNA levels in *endo^1* mutant brains. Compared to controls, the total level of *SYNJ* RNA is not affected, but Synj protein levels are reduced in *endo^1* mutant brains, suggesting that Endo stabilizes Synj protein. In addition, we did not observe a dramatic accumulation of Synj protein in motor neuron cell bodies in the ventral ganglion of *endo^1* mutants (not shown), suggesting that

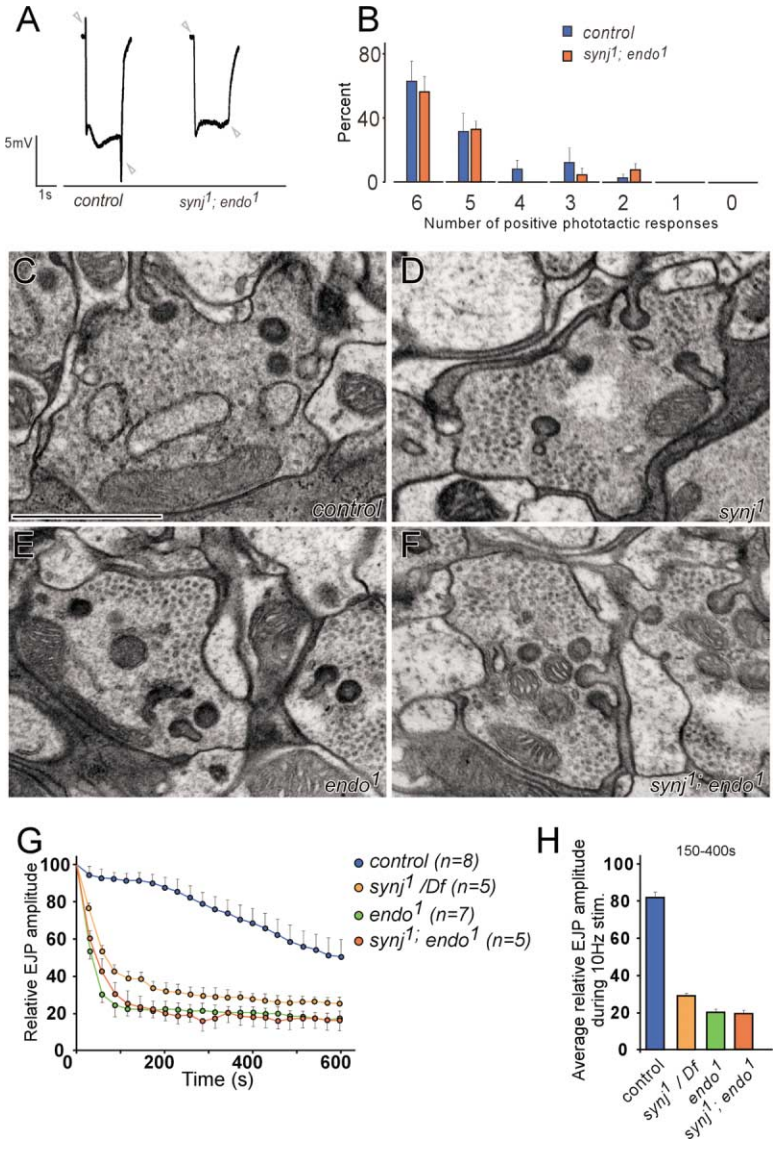

Figure 7. Double Mutant *synj*[1] and *endo*[1] Photoreceptors and NMJs Show Similar Phenotypes as Single Mutants

(A) ERG recordings from controls (*y w eyFLP; FRT42D/FRT42D cl2R w*$^+$ or *y w eyFLP; FRT82B/FRT82B cl3R w*$^+$) and flies with homozygous double mutant *synj*[1]; *endo*[1] eyes (*y w eyFLP; FRT42D synj*[1]*/FRT42D cl2R w*$^+$*; FRT82B endo*[1]*/FRT82B cl3R w*$^+$). On and off transients (or the absence thereof) are marked by arrowheads.

(B) Phototaxis assay on control flies and flies with double mutant eyes for *synj*[1] and *endo*[1]. Flies with double mutant eyes phototax as well as control flies or as flies with *synj*[1] eyes (Figure 1B) or flies with *endo*[1] eyes (Fabian-Fine et al., 2003).

(C–F) EM of control (C), *synj*[1] (D), *endo*[1] (E), and double mutant *synj*[1]; *endo*[1] (F) PR terminals. Note the appearance of densely coated vesicles in clusters. Counts of clustered vesicles show that cluster size in either *synj*[1] or *endo*[1] single mutants is not significantly different from the double mutant *synj*[1]; *endo*[1]. ($p > 0.01$ in either case; *synj*[1] [29.2 $\pm$ 3.9], *endo*[1] [47.4 $\pm$ 4.2], *synj*[1]; *endo*[1] [42.1 $\pm$ 4.8], and control [2.5 $\pm$ 1.1 clustered vesicles/μm^2]). A cluster of coated vesicles is defined as 10 or more densely coated vesicles aggregated in 3 or more rows. Scale bar equals 1 μm.

(G) Relative EJP amplitude of *synj*[1]; *endo*[1] double mutant NMJs (*yw;FRT42D synj*[1]*; FRT82B endo*[1]) stimulated at 10 Hz for 10 min (red). Data for the controls *yw; FRT42D* (shown) and *yw; FRT82B* (not shown) are not significantly different ($p > 0.01$)

(H) Average relative EJP amplitude between 150 and 450 s of stimulation for *synj*[1]; *endo*[1] double mutants is 19% of the original level (red). The difference between *endo*[1] (green) and *synj*[1]; *endo*[1] is not significantly different ($p > 0.01$).

(G and H) Data from Figures 4D and 4E are shown for comparison. Error bars indicate SEM.

Endo is not essential to target Synj to synaptic boutons of the NMJ. We therefore conclude that Endo plays a pivotal role in maintaining and stabilizing proper levels of Synj protein at synaptic terminals.

To precisely determine the localization of the residual Synj in *endo*[1] mutant boutons, we double labeled *endo*[1] mutant animals with Synj antiserum and various markers. The vesicular marker CSP is mostly localized to the synaptic membrane in *endo*[1] mutants, and it often concentrates in puncta, which likely represent AZs (Verstreken et al., 2002). Labeling of *endo*[1] boutons with CSP and Synj shows that Synj puncta are mostly interspersed between the CSP-positive puncta (Figures 9M–9P). Furthermore, labeling of *endo*[1] boutons with Synj and the AZ marker glutamate receptor IIA (Petersen et al., 1997) demonstrates that they do not colocalize (Figures 9Q–9T). Hence, we surmise that in the absence of Endo, the remaining Synj is localized to endocytotic hotspots.

Discussion

Synj Promotes Vesicle Uncoating and Regulates Vesicle-Cytomatrix Interactions

Our data indicate that Synj is essential for vesicle uncoating, in line with findings in mouse, *C. elegans*, and lamprey (Cremona et al., 1999; Gad, et al., 2000; Harris et al., 2000). Synj uncoats vesicles by dephosphorylating PI(4,5)P, thereby decreasing the affinity of clathrin adaptors to coated vesicles (McPherson et al., 1996; Cremona et al., 1999). PI(4,5)P is also implicated in organizing cytoskeletal structure. Hence, by altering phosphoinositide levels, Synj may control cytoskeletal function at endocytotic sites and regulate vesicle travel after fission (Osborne et al., 2001; Qualmann and Kessels, 2002). In line with this idea, at *synj* mutant NMJs, we observe rows of vesicles apposed to non-AZ presynaptic membrane and these vesicles are regularly spaced, and in *synj*

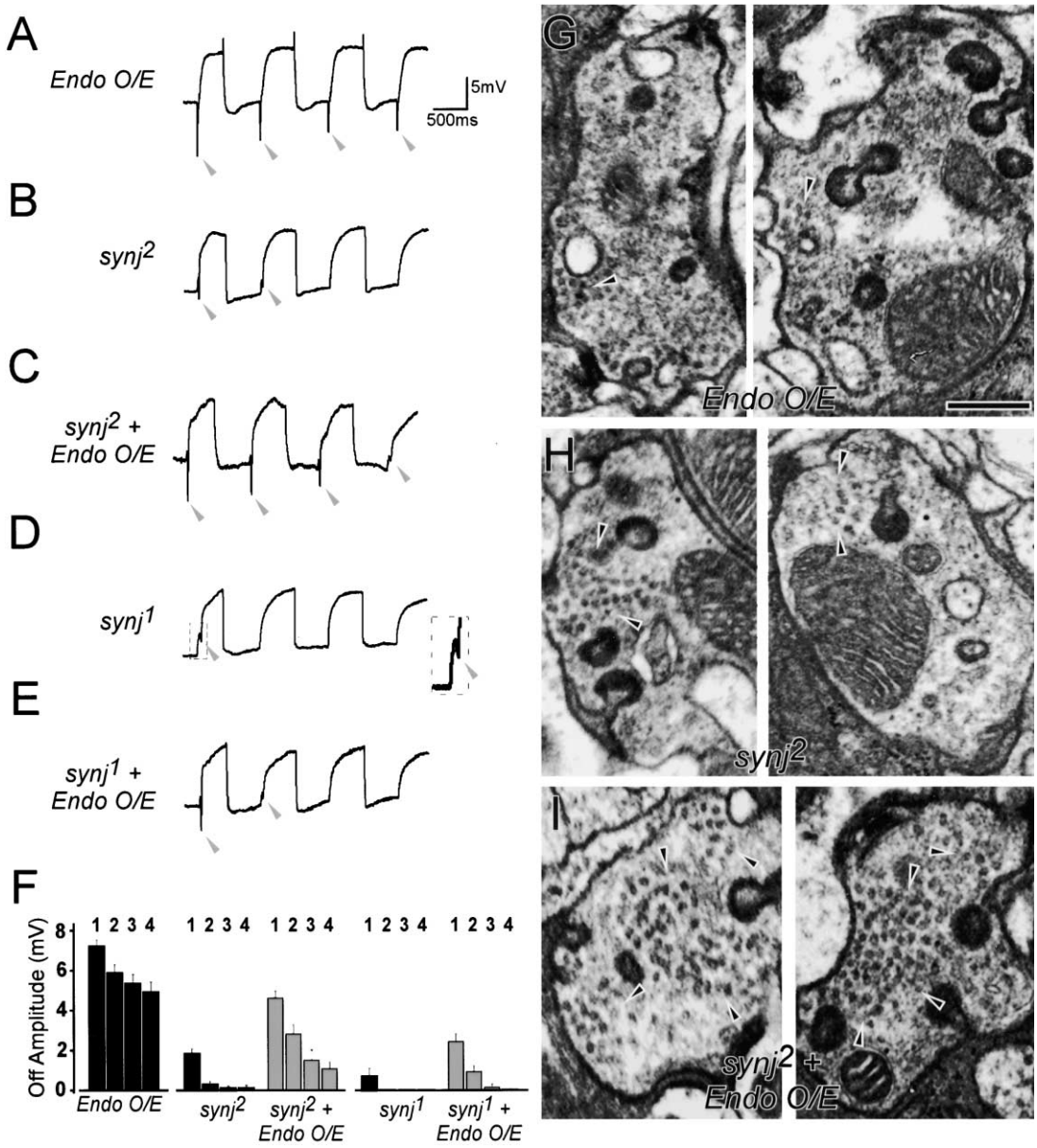

Figure 8. Overexpression of Endo Partly Rescues Partial Loss of *synj* Function

(A–E) ERG recordings, starting with "lights on," of flies overexpressing Endo in the eye (*Endo O/E: y w; FRT42D synj/CyO; ey-Gal4 UAS-FLP/ UAS-Endo^{I-III}*) (A); flies that are homozygous mutant for *synj^{1}* (D) or *synj^{2}* (B) in PRs (*y w; FRT42D synj/FRT42D cl2R GMR-hid; ey-Gal4 UAS-FLP/TM6B, Tb*); or flies that simultaneously overexpress Endo and are homozygous for *synj^{1}* (E) or *synj^{2}* (C) (*y w; FRT42D synj/FRT42D cl2R GMR-hid; ey-Gal4 UAS-FLP/UAS-Endo^{I-III}*). Off transients or delayed off transients (inset in D) are marked by an arrowhead. Note the restoration of the off transient in flies with hypomorphic *synj^{2}* mutant eyes that simultaneously overexpress Endo (compare B to C). We used the *EGUFhid* system to overexpress Endo as the *ey* promoter drives GAL4 expression weakly and shuts off in the adult eye. This avoids morphological defects associated with massive overexpression of Endo (e.g., *elav-GAL4*; P.R.H., unpublished data).

(F) The amplitudes of the four first off responses in a 500 ms light-dark stimulation protocol were quantified, $n > 8$ for each genotype. Off transient number that is quantified is indicated above the bars. Error bars indicate SEM.

(G–I) EM images of PR terminals overexpressing Endo (*Endo O/E*), *synj^{2}* mutant PR terminals, or PR terminals simultaneously overexpressing Endo and homozygous for *synj^{2}* (genotypes, see A–E). Two representative examples are shown for each genotype and arrowheads point to vesicle clusters, which are more pronounced in PRs overexpressing Endo and mutant for *synj^{2}* (I). Scale bar equals 500 nm.

mutant PR terminals, we observe clusters of densely coated and regularly spaced vesicles in multiple parallel rows, suggesting that these vesicles are associated with the cytoskeleton. Similar arrays of coated vesicles, although less pronounced, were also reported in mouse and *C. elegans synj* mutants (Harris et al., 2000; Kim et al., 2002). Hence, in mouse, nematode, and flies, the data suggest that Synj not only promotes vesicle uncoating, but that it also regulates cytoskeleton-vesicle interactions during endocytosis.

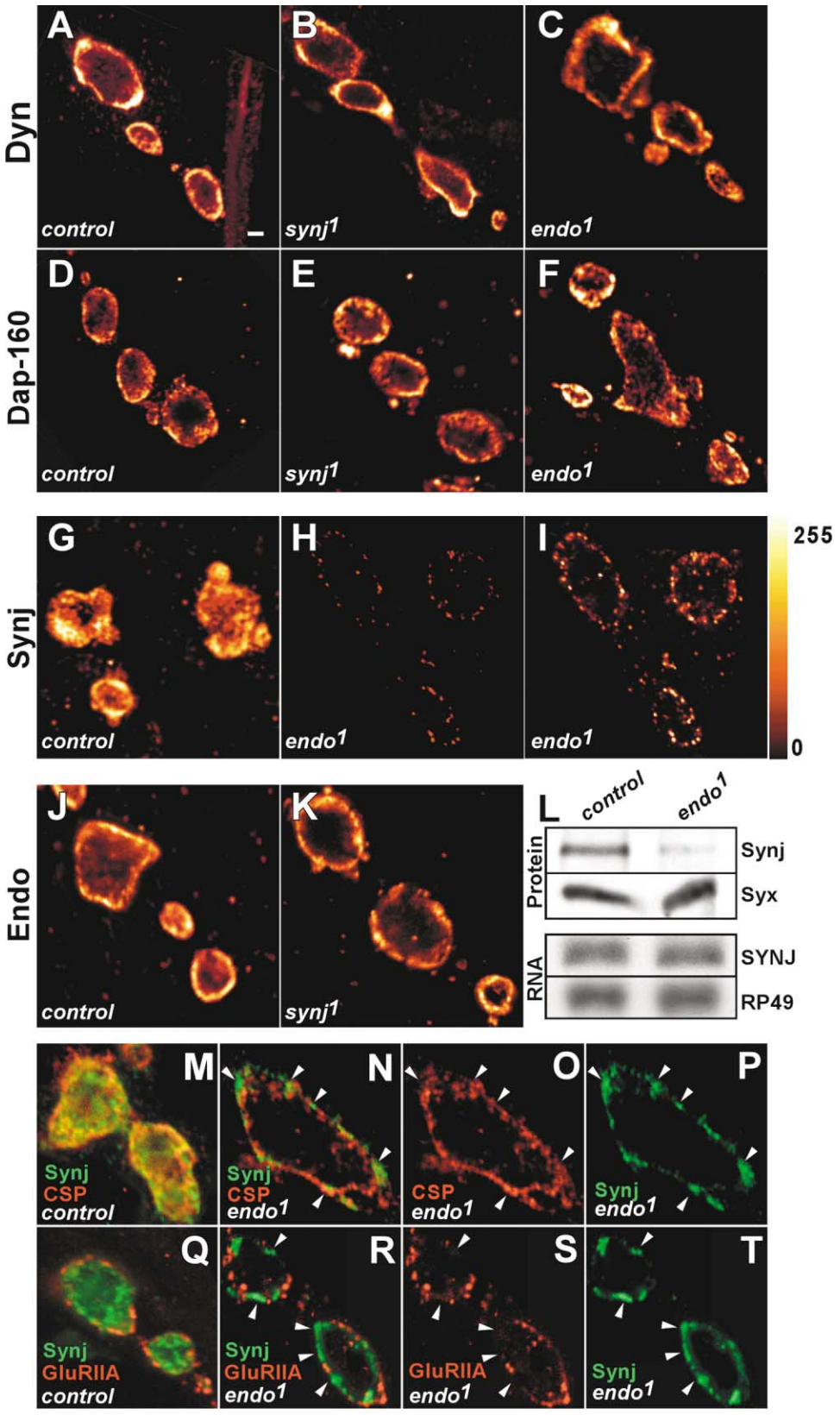

Figure 9. Endo Is Required for Stabilization and Proper Localization of Synj at the Synapse

(A–K) Labeling of control (A, D, G, and J) (*y w; FRT42D* in A, D, and G and *w* in J), *synj*^{1} (B, E, and K; *y w eyFLP; FRT42D synj*^{1}), and *endo*^{1} (C, F, H, and I; *w; endo*^{1}) NMJ boutons of third instar larvae with anti-Dynamin monoclonal antibody (A–C); anti-Dap160 antibody (D–F); anti-Synj antibody (G–I); or anti-Endo antibody (J and K). Labeling in (G) and (H) was performed in the same tube and images were acquired using the

Synj and Endo Are Required for a Late Endocytotic Step

The biochemical activities of Synj and Endo suggest that these two proteins act at distinct steps in endocytosis. Endo is thought to alter membrane curvature, leading to deformation of the presynaptic membrane during early endocytosis (Schmidt et al., 1999). If Endo and Synj act at distinct steps, we expect the individual mutants to display different phenotypes. However, at PR terminals with mutations in either *endo* or *synj*, we observe almost identical phenotypes, indicating that Synj and Endo function are ultimately required at the same step in endocytosis (this work; Fabian-Fine et al., 2003).

Interestingly, *C. elegans synj* null synapses and hypomorphic *endo* NMJs show early endocytotic intermediates (Guichet et al., 2002; Harris et al., 2000). In addition, in *Drosophila*, the total vesicle number at $synj^1$ or $endo^1$ NMJs is far lower than in controls, suggesting that Endo or Synj might also affect early endocytotic steps. However, $synj^1$ and $endo^1$ NMJs do show regularly spaced coated vesicles away from the AZs, suggesting that Synj and Endo function is essential later in endocytosis. Similarly, at *synj* or *endo* mutant PR terminals, clusters of coated vesicles accumulate in large numbers, further supporting a late role in endocytosis. Hence, while we do not rule out a role for Synj or Endo during early endocytotic steps at some synapses, our data indicate that both Synj and Endo are ultimately required for the uncoating of newly internalized SVs at both NMJs as well as PR terminals.

Synj and Endo Are Functional Partners in Endocytosis

In line with previous studies, we show here that in *Drosophila*, Synj and Endo bind to one another, even in the absence of SVs. In addition, we present data indicating that Synj and Endo are important for endocytosis at the coated vesicle stage, in agreement with Gad et al. (2000), and we provide genetic evidence that Endo and Synj interact in vivo. Specifically, *synj* and *endo* single and double mutants display dramatically similar phenotypes in ultrastructural and functional assays, and overexpression of Endo in PRs partially alleviates the functional defects of a hypomorphic *synj* mutant, suggesting that Endo acts upstream of Synj. We also show that in $endo^1$ null mutants, Synj is mislocalized and destabilized. Thus, our data not only indicate that the functional interaction between Synj and Endo is important for vesicle uncoating, they also indicate that a key function of Endo is to stabilize and localize Synj within the nerve terminal. Taken together, the data allow us to propose a model for the function of Endo and Synj in SV endocytosis. Before vesicle invagination, Synj is tethered to endocytotic zones, perhaps through its interaction with Dap160. Endo binds the Synj proline-rich domain and recruits it to newly forming vesicles, where it is stabilized by its interaction with Endo. After vesicle fission, stabilized Synj catalyzes SV uncoating. The precise regulatory mechanisms that delay uncoating by Synj until after vesicle fission are unknown, but it is interesting to note that Synj undergoes dephosphorylation in response to persistent or high-frequency membrane depolarization (Cousin et al., 2001). However, it remains to be determined whether this modification actually regulates Synj function in vivo.

Kiss-and-Run versus Clathrin-Mediated Endocytosis

Different modes of vesicle recycling exist at synapses (Aravanis et al., 2003; Kjaerulff et al., 2002). Our data from $endo^1$ mutant NMJs indicate the existence of at least two different types of vesicle recycling (Verstreken et al., 2002), and the data presented here are consistent with this idea. First, clear SVs are almost entirely depleted from $synj^1$ mutant NMJ boutons, but small vesicle clusters remain at AZs, suggesting that they undergo rapid recycling during stimulation. Second, by disrupting clathrin-mediated endocytosis, neurotransmitter release at *synj* and *endo* single or double mutant NMJs undergoes depression during intense stimulation but is maintained at a stable level during low-frequency stimulation, in agreement with the observation that vesicle recycling modes change with stimulation frequency (Sun et al., 2002). Third, dye uptake during prolonged stimulation is severely reduced in *synj* mutants; note here that we have used FM1-43, which labels SVs undergoing clathrin-mediated endocytosis but does not label SVs involved in kiss-and-run (Klingauf et al., 1998; Verstreken et al., 2002). Fourth, ERG on/off transients recorded from flies with $synj^1$, $synj^2$, or $endo^1$ single mutant or double mutant eyes are absent or severely reduced, but the flies phototax normally, suggesting that some vesicle recycling persists. In conclusion, the data are in agreement with and further support the idea that kiss-and-run maintains some neurotransmitter release when clathrin-mediated endocytosis is blocked or severely impaired. Finally, labeling of $endo^1$ mutant boutons with anti-Synj and an AZ marker demonstrates that both markers are mutually exclusive, indicating that kiss-and-run, which operates at the AZ in $endo^1$ mutants, is spatially separated from the area where clathrin-mediated endocytosis occurs. It is worth mentioning that the kiss-and-run mode of release may also play an important role in mouse synapses that are depleted of *synaptojanin-1*, as they exhibit many of the features that we observe at mutant NMJs and PR terminals (Cremona et al., 1999; Kim et al., 2002).

Experimental Procedures

Drosophila Strains and Genetics

Mutagenesis: *y w/Y; P{ry$^+$ neoFRT}42D^{isogenized}* males were fed 15 mM EMS and crossed to *y w P{ry$^+$ ey-FLP.N}2, P{GMR-lacZ.C(38.1)}TPN1;*

same settings. The gain was increased in (I) compared to (H). Single confocal sections are shown throughout the figure.

(L) (Top) Immunoblot of control and $endo^1$ third instar brain extract, probed with anti-Synj and anti-Syntaxin (Syx) as a control. (Bottom) Northern blot of control and $endo^1$ third instar larvae probed with *synj* and *RP49* as a control.

(M–T) Double labeling of Synj (green) and CSP (red; M–P) or GluRIIA (red; Q–T) on control (*w*) and $endo^1$ mutant boutons. Note the mutually exclusive localization of Synj and these markers. Scale bar in (A) is 2 μm for (A)–(K) and 660 nm for (M)–(T).

P{ry⁺ neoFRT}42D, P{w⁺ ry⁺white-un1}47A l(2)cl-R11¹/CyO-KrGFP (Newsome et al., 2000) to create F1 flies homozygous for *2R* in the majority of PRs. Hereafter, we will refer to *P{ry⁺ neoFRT}42D* and *P{ry⁺ neoFRT}82B* as *FRT42D* and *FRT82B*, respectively. Of the 43,707 male flies screened, 3,081 flies failed or partly failed to phototax and were retained. In total, we established 118 stocks on *2R* with an ERG defect; 92 are homozygous lethal. Complementation tests reveal 14 complementation groups with 2 or more alleles.

For rescue experiments, we used cosmid[1–12] and cosmid[1–5] described in Kerrebrock et al. (1995). Presence of the *synj* gene in the cosmids was confirmed by Southern and PCR. Insert ends were defined by Southern and sequencing. The lethality and ERG phenotype of *synj¹*, *synj¹/synj²*, and *synj²* were rescued by the cosmids; however, we obtained fewer *synj²* rescued animals, likely due to a second nonessential hit in *arc* on the *synj²* chromosome.

synj¹, *synj²*, and *Df(2R)R1-8* are maintained over *CyO-KrGFP*, and mutant animals were obtained by growing 10–50 non-GFP animals per grape juice plate with liquid yeast paste. *endo¹* is maintained over *TM6B*, *Tb¹*, and homozygous mutants are selected by non-*Tubby* appearance. Animals double mutant for *synj¹* and *endo¹* were selected from: *y w; T(2;3)CyO-TM6,CyO:TM6B, Tb¹/ FRT42D synj¹/ CyO; FRT82B endo¹/TM6B, Tb¹*.

Flies with eyes double mutant for *synj¹* and *endo¹* were obtained by crossing *y w/Y; FRT42D synj¹/CyO; FRT82B endo¹/TM6B* males to *y w P{ry⁺ ey-FLP.N}2, P{GMR-lacZ.C(38.1)}TPN1; FRT42D, P{w⁺ ry⁺ white-un1}47A l(2)cl-R11¹/CyO; FRT82B, P{w⁺ ry⁺ white-un1}90E l(3)cl-R3¹/TM3, Sb*.

Controls for *eyFLP* experiments were *y w P{ry⁺ ey-FLP.N}2, P{GMR-lacZ.C(38.1)}TPN1; FRT42D/P{ry⁺ neoFRT}42D, P{w⁺ ry⁺ white-un1}47A l(2)cl-R11¹* unless otherwise indicated. Controls for NMJ experiments were *y w*; *FRT42D* larvae unless otherwise indicated. Controls were of similar size as mutants; about 3.5 mm in length for *synj¹* and *synj²* and about 1.5 to 2 mm for *endo¹* and *synj1;endo1* larvae.

Flies that overexpress Endo in *synj¹* or *synj²* mutant PRs were obtained by crossing *y w/Y; FRT42D synj¹/CyO; P{w⁺, UAS-endo$^{I\text{-}III}$}/ TM6B, Tb¹* to *y w; FRT42D, P{y⁺ ry⁺ Car20y}44B, P{w⁺ GMR-hid} SS2, l(2)CL-R¹/CyO; P{w⁺ GAL4-ey.H}SS5, P{w⁺ UAS-FLP1.D}JD2* (Stowers and Schwarz, 1999). Out of this cross, *y w*; *FRT42D synj¹/ P{ry⁺ neoFRT}42D, P{y⁺ ry⁺ Car20y}44B, P{w⁺ GMR-hid}SS2 l(2)CL-R¹; P{w⁺ GAL4-ey.H}SS5, P{w⁺ UAS-FLP1.D}JD2/P{w⁺, UAS-endo$^{I\text{-}III}$}* flies overexpress Endo and are homozygous mutant for *synj¹* in their eyes (*synj¹ + Endo O/E*). *y w; FRT42D synj¹/FRT42D, P{y⁺ ry⁺ Car20y}44B, P{w⁺ GMR-hid}SS2, l(2)CL-R¹; P{w⁺ GAL4-ey.H}SS5, P{w⁺ UAS-FLP1.D}JD2/TM6B, Tb¹* are homozygous mutant for *synj¹* (*synj¹*). *y w; FRT42D synj¹/CyO; P{w⁺, UAS-endo$^{I\text{-}III}$}/P{w⁺ GAL4-ey.H}SS5, P{w⁺ UAS-FLP1.D}JD2* overexpress Endo in the eyes (*Endo O/E*). Similar crosses were set to obtain flies that overexpress Endo and are mutant for *synj²* in their eyes.

Phototaxis Assays

Phototaxis assays (Benzer, 1967) were performed as described in the Supplemental Data (http://www.neuron.org/cgi/content/full/40/4/733/DC1). Some mutants isolated in our screen were blind or partially blind when tested during screening but are not blind several generations later. We surmise that this discrepancy is due to genetic load resulting from EMS treatment, resulting in impaired sight and decreased ability to phototax. However, several generations later, unlinked lesions segregate randomly, resulting in improved sight and normal phototaxis.

Molecular Biology and Biochemistry

synj¹ and *synj²* alleles were sequenced in *trans* over an isogenized chromosome using standard techniques. *synj²* was also sequenced over *Df(2R)R1-8*. UAS-*endo* and GST-synjPRD were generated, and GST-synjPRD and GST-Dap160 SH3 were expressed as outlined in the Supplemental Data (http://www.neuron.org/cgi/content/full/40/4/733/DC1). Rabbit antibodies against GST-SynjPRD (pAb3072) were raised at Alpha Diagnostics (San Antonio, TX) and purified as described (Roos and Kelly, 1998).

Details on IP experiments, GST-pull-down assays, and preparation of SV and cytosolic fractions (Schulze et al., 1995) are described in the Supplemental Data.

Antibody dilutions used on Western blots: anti-Synj, 1:5000; guinea pig anti-Endo (GP69), 1:5000; Rat anti-Endo (R44), 1:7500 (Verstreken et al., 2002); anti-Dap160 (pAb1704), 1:10,000 (Roos and Kelly, 1998); anti-Dyn (pAb2074), 1:5000 (Roos and Kelly, 1998); anti-Syb (R29), 1:5000 (Wu et al., 1999); anti-CSP (mAb 49), 1:1000 (Zinsmaier et al., 1994); anti-ROP (4F8), 1:10,000 (Wu et al., 1999); anti-Syx (8C6), 1:2000 (Schulze et al., 1995); secondary HRP-conjugated antibodies, 1:5000.

Immunocytochemistry

Larvae and adult brains were fixed in 3.5% formaldehyde (FA) for 20 min and washed in 0.1% Tween-20 (larvae) or 0.4% Triton X-100 (brains). For GluRIIA labeling, larvae were fixed in 50% picric acid, 2.5% FA in PBS for 15 min and washed in 0.4% Triton X 100. To deplete vesicles, *shi^{ts1}* larvae were dissected and incubated at 35°C for 20 min in HL3 with 60 mM KCl and fixed at 35°C. Antibody dilutions used: Synj (pAb3072), 1:200; Endo (GP69), 1:200; 24B10, 1:50 (Van Vactor et al., 1988); CSP, 1:50; DVAP-33A, 1:200 (Pennetta et al., 2002); Dap160 (pAb1704), 1:200; Dynamin (mAb clone 41), 1:50 (BD Transduction Labs); GluRIIA, 1:50 (Petersen et al., 1997). Secondary antibodies conjugated to Cy3, Cy5, or Alexa 488 (Jackson Immunolabs, Molecular Probes) were used at 1:250. Images were captured with a Zeiss 510 confocal microscope and processed with Amira 2.2 and Adobe Photoshop 7.0.

Electrophysiology and FM1-43 Dye Uptake

ERGs were recorded as described in the Supplemental Data (http://www.neuron.org/cgi/content/full/40/4/733/DC1) (Fabian-Fine et al., 2003; Heisenberg, 1971).

Third instar larval muscle recordings were performed as described in Supplemental Data (Verstreken et al., 2002). Larvae were dissected and recordings were performed in modified HL3 (in mM): NaCl (110), KCl (5), $NaHCO_3$ (10), HEPES (5), sucrose (30), trehalose (5), $CaCl_2$ (5), and $MgCl_2$ (20) (pH 7.2).

FM1-43 dye uptake was performed as described (Verstreken et al., 2002). Dye uptake was monitored with a BioRad confocal microscope. Equidistant confocal slices were scanned and the average pixel intensity in the entire 3D bouton was determined using the segmentation editor in Amira 2.2. Background in the muscle was subtracted from bouton labeling. Data was normalized to the average labeling intensity in controls.

Transmission Electron Microscopy (TEM)

TEM preparation of adult eye laminae were performed as described (Fabian-Fine et al., 2003). 1-day-old flies were dissected and fixed at 4°C in 2% para-FA; 2% glutaraldehyde; 0.1 M Na-cacodylate; 0.005% $CaCl_2$ (pH 7.2) and postfixed in 2% OsO_4. 50 nm thin sections were stained in 4% uranyl acetate and 2.5% lead nitrate. Synaptic features of laminae were scored double-blind by several observers. Larvae were dissected in fixative, prepared for TEM, and quantified as described (Verstreken et al., 2002). Throughout the paper, two-tailed Student's t tests were used to compare data.

Acknowledgments

We thank E. Seto and K. Venken for comments and members of the Bellen lab for discussions. We thank R. Nolo, O. Kjærulff, and H. Fotowat for their help, and L. Clift-O'Grady, R. Kelly, G. Halder, B.D.G.P., Bloomington Stock Center, and the University of Iowa Hybridoma Bank for reagents. P.V. is supported by the BAEF; K.L.S., R.G.Z., P.R.H., and H.J.B. are supported by the HHMI; and P.R.H. by the EMBO. This work was supported by NIH grant NS15927 to R. Kelly and J.R. H.J.B. is an HHMI Investigator.

Received: June 20, 2003
Revised: August 26, 2003
Accepted: September 22, 2003
Published: November 12, 2003

References

Aravanis, A.M., Pyle, J.L., and Tsien, R.W. (2003). Single synaptic vesicles fusing transiently and successively without loss of identity. Nature *423*, 643–647.

Benzer, S. (1967). Behavioral mutants of *Drosophila* isolated by countercurrent distribution. Proc. Natl. Acad. Sci. USA *58*, 1112–1119.

Betz, W.J., and Bewick, G.S. (1992). Optical analysis of synaptic vesicle recycling at the frog neuromuscular junction. Science *255*, 200–203.

Burg, M.G., Sarthy, P.V., Koliantz, G., and Pak, W.L. (1993). Genetic and molecular identification of a *Drosophila* histidine decarboxylase gene required in photoreceptor transmitter synthesis. EMBO J. *12*, 911–919.

Cousin, M.A., Tan, T.C., and Robinson, P.J. (2001). Protein phosphorylation is required for endocytosis in nerve terminals: potential role for the dephosphins dynamin I and synaptojanin, but not AP180 or amphiphysin. J. Neurochem. *76*, 105–116.

Cremona, O., Di Paolo, G., Wenk, M.R., Luthi, A., Kim, W.T., Takei, K., Daniell, L., Nemoto, Y., Shears, S.B., Flavell, R.A., et al. (1999). Essential role of phosphoinositide metabolism in synaptic vesicle recycling. Cell *99*, 179–188.

Fabian-Fine, R., Verstreken, P., Hiesinger, P.R., Horne, J.A., Kostyleva, R., Zhou, Y., Bellen, H.J., and Meinertzhagen, I.A. (2003). Endophilin promotes a late step in endocytosis at glial invaginations in *Drosophila* photoreceptor terminals. J. Neurosci., in press.

Gad, H., Ringstad, N., Low, P., Kjaerulff, O., Gustafsson, J., Wenk, M., Di Paolo, G., Nemoto, Y., Crun, J., Ellisman, M.H., et al. (2000). Fission and uncoating of synaptic clathrin-coated vesicles are perturbed by disruption of interactions with the SH3 domain of endophilin. Neuron *27*, 301–312.

Gonzalez-Gaitan, M., and Jackle, H. (1997). Role of *Drosophila* alpha-adaptin in presynaptic vesicle recycling. Cell *88*, 767–776.

Guichet, A., Wucherpfennig, T., Dudu, V., Etter, S., Wilsch-Brauniger, M., Hellwig, A., Gonzalez-Gaitan, M., Huttner, W.B., and Schmidt, A.A. (2002). Essential role of endophilin A in synaptic vesicle budding at the *Drosophila* neuromuscular junction. EMBO J. *21*, 1661–1672.

Harris, T.W., Hartwieg, E., Horvitz, H.R., and Jorgensen, E.M. (2000). Mutations in synaptojanin disrupt synaptic vesicle recycling. J. Cell Biol. *150*, 589–600.

Heisenberg, M. (1971). Separation of receptor and lamina potentials in the electroretinogram of normal and mutant *Drosophila*. J. Exp. Biol. *55*, 85–100.

Hurley, J.H., and Wendland, B. (2002). Endocytosis: driving membranes around the bend. Cell *111*, 143–146.

Kerrebrock, A.W., Moore, D.P., Wu, J.S., and Orr-Weaver, T.L. (1995). Mei-S332, a *Drosophila* protein required for sister-chromatid cohesion, can localize to meiotic centromere regions. Cell *83*, 247–256.

Kim, W.T., Chang, S., Daniell, L., Cremona, O., Di Paolo, G., and De Camilli, P. (2002). Delayed reentry of recycling vesicles into the fusion-competent synaptic vesicle pool in synaptojanin 1 knockout mice. Proc. Natl. Acad. Sci. USA *99*, 17143–17148.

Kjaerulff, O., Verstreken, P., and Bellen, H.J. (2002). Synaptic vesicle retrieval: still time for a kiss. Nat. Cell Biol. *4*, E245–E248.

Klingauf, J., Kavalali, E.T., and Tsien, R.W. (1998). Kinetics and regulation of fast endocytosis at hippocampal synapses. Nature *394*, 581–585.

Klyachko, V.A., and Jackson, M.B. (2002). Capacitance steps and fusion pores of small and large-dense-core vesicles in nerve terminals. Nature *418*, 89–92.

Koenig, J.H., and Ikeda, K. (1989). Disappearance and reformation of synaptic vesicle membrane upon transmitter release observed under reversible blockage of membrane retrieval. J. Neurosci. *9*, 3844–3860.

Lloyd, T.E., Verstreken, P., Ostrin, E.J., Phillippi, A., Lichtarge, O., and Bellen, H.J. (2000). A genome-wide search for synaptic vesicle cycle proteins in *Drosophila*. Neuron *26*, 45–50.

McPherson, P.S., Garcia, E.P., Slepnev, V.I., David, C., Zhang, X., Grabs, D., Sossin, W.S., Bauerfeind, R., Nemoto, Y., and De Camilli, P. (1996). A presynaptic inositol-5-phosphatase. Nature *379*, 353–357.

Meinertzhagen, I.A., and Sorra, K.E. (2001). Synaptic organization in the fly's optic lamina: few cells, many synapses and divergent microcircuits. Prog. Brain Res. *131*, 53–69.

Newsome, T.P., Asling, B., and Dickson, B.J. (2000). Analysis of *Drosophila* photoreceptor axon guidance in eye-specific mosaics. Development *127*, 851–860.

Osborne, S.L., Meunier, F.A., and Schiavo, G. (2001). Phosphoinositides as key regulators of synaptic function. Neuron *32*, 9–12.

Pennetta, G., Hiesinger, P., Fabian-Fine, R., Meinertzhagen, I., and Bellen, H. (2002). *Drosophila* VAP-33A directs bouton formation at neuromuscular junctions in a dosage-dependent manner. Neuron *35*, 291–306.

Petersen, S.A., Fetter, R.D., Noordermeer, J.N., Goodman, C.S., and DiAntonio, A. (1997). Genetic analysis of glutamate receptors in *Drosophila* reveals a retrograde signal regulating presynaptic transmitter release. Neuron *19*, 1237–1248.

Qualmann, B., and Kessels, M.M. (2002). Endocytosis and the cytoskeleton. Int. Rev. Cytol. *220*, 93–144.

Rikhy, R., Kumar, V., Mittal, R., and Krishnan, K.S. (2002). Endophilin is critically required for synapse formation and function in *Drosophila melanogaster*. J. Neurosci. *22*, 7478–7484.

Ringstad, N., Nemoto, Y., and De Camilli, P. (1997). The SH3p4/Sh3p8/SH3p13 protein family: binding partners for synaptojanin and dynamin via a Grb2-like Src homology 3 domain. Proc. Natl. Acad. Sci. USA *94*, 8569–8574.

Roos, J., and Kelly, R.B. (1998). Dap160, a neural-specific Eps15 homology and multiple SH3 domain-containing protein that interacts with *Drosophila* dynamin. J. Biol. Chem. *273*, 19108–19119.

Sakisaka, T., Itoh, T., Miura, K., and Takenawa, T. (1997). Phosphatidylinositol 4,5-bisphosphate phosphatase regulates the rearrangement of actin filaments. Mol. Cell. Biol. *17*, 3841–3849.

Sankaranarayanan, S., Atluri, P.P., and Ryan, T.A. (2003). Actin has a molecular scaffolding, not propulsive, role in presynaptic function. Nat. Neurosci. *6*, 127–135.

Schmidt, A., Wolde, M., Thiele, C., Fest, W., Kratzin, H., Podtelejnikov, A.V., Witke, W., Huttner, W.B., and Soling, H.D. (1999). Endophilin I mediates synaptic vesicle formation by transfer of arachidonate to lysophosphatidic acid. Nature *401*, 133–141.

Schulze, K.L., Broadie, K., Perin, M.S., and Bellen, H.J. (1995). Genetic and electrophysiological studies of *Drosophila* syntaxin-1A demonstrate its role in nonneuronal secretion and neurotransmission. Cell *80*, 311–320.

Slepnev, V.I., and De Camilli, P. (2000). Accessory factors in clathrin-dependent synaptic vesicle endocytosis. Nat. Rev. Neurosci. *1*, 161–172.

Stowers, R.S., and Schwarz, T.L. (1999). A genetic method for generating *Drosophila* eyes composed exclusively of mitotic clones of a single genotype. Genetics *152*, 1631–1639.

Sun, J.Y., Wu, X.S., and Wu, L.G. (2002). Single and multiple vesicle fusion induce different rates of endocytosis at a central synapse. Nature *417*, 555–559.

Takei, K., and Haucke, V. (2001). Clathrin-mediated endocytosis: membrane factors pull the trigger. Trends Cell Biol. *11*, 385–391.

van de Goor, J., Ramaswami, M., and Kelly, R. (1995). Redistribution of synaptic vesicles and their proteins in temperature-sensitive shibire(ts1) mutant *Drosophila*. Proc. Natl. Acad. Sci. USA *92*, 5739–5743.

Van Vactor, D., Jr., Krantz, D.E., Reinke, R., and Zipursky, S.L. (1988). Analysis of mutants in chaoptin, a photoreceptor cell-specific glycoprotein in Drosophila, reveals its role in cellular morphogenesis. Cell *52*, 281–290.

Verstreken, P., Kjaerulff, O., Lloyd, T.E., Atkinson, R., Zhou, Y., Meinertzhagen, I.A., and Bellen, H.J. (2002). Endophilin mutations block clathrin-mediated endocytosis but not neurotransmitter release. Cell *109*, 101–112.

Wu, M.N., Fergestad, T., Lloyd, T.E., He, Y., Broadie, K., and Bellen, H.J. (1999). Syntaxin 1A interacts with multiple exocytic proteins to regulate neurotransmitter release in vivo. Neuron *23*, 593–605.

Zhai, R.G., Hiesinger, P.R., Koh, T.-W., Verstreken, P., Schulze, K.L., Cao, Y., Jafar-Nejad, H., Norga, K.K., Pan, H., Bayat, V., et al. (2003).

Mapping *Drosophila* mutantions with molecularly defined P-element insertions. Proc. Natl. Acad. Sci. USA *100*, 10860–10865.

Zinsmaier, K.E., Eberle, K.K., Buchner, E., Walter, N., and Benzer, S. (1994). Paralysis and early death in cysteine string protein mutants of *Drosophila*. Science *263*, 977–980.

Note Added in Proof

Schuske et al. (this issue of *Neuron*) isolated *C. elegans* endophilin mutants and investigated the in vivo interaction between endophilin and synaptojanin. They found independently that a major role for endophilin is to serve as an adaptor for Synaptojanin, stabilizing its expression at the synapse, thereby promoting vesicle uncoating. For further reading, see Schuske, K.R., Richmond, J.E., Matthies, D.S., Davis, W.S., Runz, S., Rube, D.A., van der Bliek, A.M., and Jorgensen, E.M. (2003). Endophilin is required for synaptic vesicle endocytosis by localizing synaptojanin. Neuron *40*, 749–762.